

AD-A054 616

AEROSPACE CORP EL SEGUNDO CALIF IVAN A GETTING LABS

F/G 20/5

SIMPLIFIED MODEL OF A CW DIFFUSION-TYPE CHEMICAL LASER - AN EXT--ETC(U)

APR 78 H MIRELS

F04701-77-C-0078

UNCLASSIFIED

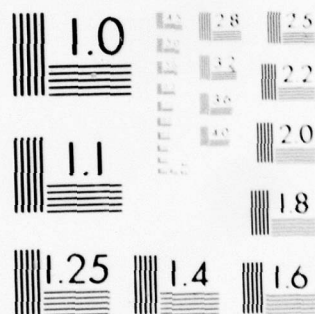
TR-0078(3940-01)-3

SAMSO-TR-78-83

NL

1 of 1
AD
A054616





MICROCOPY RESOLUTION TEST CHART
NATIONAL BUREAU OF STANDARDS-1963-A

FOR FURTHER TRAN

REPORT SAMSO-TR-78-83

2
F

AD A 05 4616
**Simplified Model of a CW Diffusion-Type Chemical Laser —
An Extension**

HAROLD MIRELS
Aerophysics Laboratory ✓
→ The Ivan A. Getting Laboratories
The Aerospace Corporation
El Segundo, Calif. 90245

7 April 1978

Interim Report

APPROVED FOR PUBLIC RELEASE;
DISTRIBUTION UNLIMITED

DDC
RECEIVED
JUN 1 1978
B

Prepared for
SPACE AND MISSILE SYSTEMS ORGANIZATION
AIR FORCE SYSTEMS COMMAND
Los Angeles Air Force Station
P.O. Box 92960, Worldway Postal Center
Los Angeles, Calif. 90009

AD No. _____
DDC FILE COPY

This interim report was submitted by The Aerospace Corporation, El Segundo, CA 90245, under Contract No. F04701-77-C-0078 with the Space and Missile Systems Organization, Deputy for Advanced Space Programs, P.O. Box 92960, Worldway Postal Center, Los Angeles, CA 90009. It was reviewed and approved for The Aerospace Corporation by W. R. Warren, Jr., Director, Aerophysics Laboratory. Lieutenant Dara Batki, SAMSO/YCPT, was the project officer for Advanced Space Programs.

This report has been reviewed by the Information Office (OI) and is releasable to the National Technical Information Service (NTIS). At NTIS, it will be available to the general public, including foreign nations.

This technical report has been reviewed and is approved for publication. Publication of this report does not constitute Air Force approval of the report's findings or conclusions. It is published only for the exchange and stimulation of ideas.

Dara Batki

Dara Batki, Lt, USAF
Project Officer

Robert W. Lindemuth

Robert W. Lindemuth, Lt Col, USAF
Chief, Technology Plans Division

FOR THE COMMANDER

Floyd R. Stuart

FLOYD R. STUART, Col, USAF
Deputy for Advanced Space
Programs

UNCLASSIFIED

SECURITY CLASSIFICATION OF THIS PAGE (When Data Entered)

18 19 REPORT DOCUMENTATION PAGE		READ INSTRUCTIONS BEFORE COMPLETING FORM
1. REPORT NUMBER SAMS0 TR-78-83	2. GOVT ACCESSION NO.	3. RECIPIENT'S CATALOG NUMBER 9
4. TITLE (and Subtitle) SIMPLIFIED MODEL OF A CW DIFFUSION- TYPE CHEMICAL LASER - AN EXTENSION.		5. TYPE OF REPORT & PERIOD COVERED Interim rept.
6. PERFORMING ORG. REPORT NUMBER TR-0078(3940-01)-3		7. CONTRACT OR GRANT NUMBER(s) F04701-77-C-0078
7. AUTHOR(s) Harold Mirels	8. PERFORMING ORGANIZATION NAME AND ADDRESS The Aerospace Corporation El Segundo, Calif. 90245	9. PROGRAM ELEMENT, PROJECT, TASK AREA & WORK UNIT NUMBERS
10. CONTROLLING OFFICE NAME AND ADDRESS Space and Missile Systems Organization Air Force Systems Command Los Angeles, Calif. 90045	11. REPORT DATE 7 Apr 1978	12. NUMBER OF PAGES 55
13. MONITORING AGENCY NAME & ADDRESS (if different from Controlling Office) 12 59p.	14. SECURITY CLASS. (of this report) Unclassified	15. DECLASSIFICATION/DOWNGRADING SCHEDULE
16. DISTRIBUTION STATEMENT (of this Report) Approved for public release; distribution unlimited.		
17. DISTRIBUTION STATEMENT (of the abstract entered in Block 20, if different from Report)		
18. SUPPLEMENTARY NOTES		
19. KEY WORDS (Continue on reverse side if necessary and identify by block number) Chemical Laser Laser Scaling Reactive Flows		
20. ABSTRACT (Continue on reverse side if necessary and identify by block number) The simplified two-vibrational-level model of a cw diffusion-type chemical laser presented by Mirels, Hofland, and King is extended to include multiple vibrational levels. Both laminar and turbulent diffusion are considered. Expressions for axial gain distribution and net output power from a Fabry-Perot optical resonator are deduced. For a given lasing species, the resulting cw chemical laser scaling laws are the same as those previously deduced by Mirels, Hofland, and King, except for the dependence of certain coefficients on rotational quantum number J and temperature T. Broadwell		

DD FORM 1473
(FACSIMILE)

409 944

UNCLASSIFIED LB
SECURITY CLASSIFICATION OF THIS PAGE (When Data Entered)

UNCLASSIFIED

SECURITY CLASSIFICATION OF THIS PAGE(When Data Entered)

19. KEY WORDS (Continued)

20. ABSTRACT (Continued)

previously presented a multiple-vibrational-level model for a cw chemical laser that was limited, however, to turbulent diffusion. The flame-sheet-mixing model used in the present study is shown to give results that are identical with those from the scheduled-mixing model of Broadwell when mean chemical rates are used.

UNCLASSIFIED

SECURITY CLASSIFICATION OF THIS PAGE(When Data Entered)

PREFACE

This work was partly supported during FY 75 by the Naval Research Laboratory through U.S. Air Force Space and Missile Systems Organization (SAMSO) Contract No. F04701-74-C-0075.

ACCESSION for	
NTIS	White Section <input checked="" type="checkbox"/>
DDC	Soft Section <input type="checkbox"/>
UNANNOUNCED	<input type="checkbox"/>
JUSTIFICATION	
BY	
DISTRIBUTION/AVAILABILITY CODES	
Dist.	AVAIL. STD./or SPECIAL
A	

CONTENTS

PREFACE	1
I. INTRODUCTION	5
II. THEORY	7
A. Basic Equations	7
B. Zero-Power and Amplifier Cases	14
C. Oscillator Cases	17
Table 1. Parameters for Defining Oscillator Performance for Cold-Reaction HF Lasers	27
III. DISCUSSION OF RESULTS	31
IV. CONCLUDING REMARKS	37
APPENDIXES	
A. Reaction Model	39
B. Zero-Power Number Density Distribution	47
C. Mixing Models	49
REFERENCES	53
SYMBOLS	55

FIGURES

1.	Mixing Model of Mirels, Hofland, and King	8
2.	Zero-Power Number Density and Gain Distribution for Cold-Reaction HF Laser	16
3.	Saturated Laser Performance for $K_1 \rightarrow \infty$ and $m = 1/2$, [Eqs. (30)]	26
4.	Effect of J Variation on Output Power from Cold- Reaction HF Chemical Laser	28
5.	Mixing Model of Broadwell	36

I. INTRODUCTION

Various approaches have been taken to analyze theoretically the performance of cw diffusion-type HF/DF chemical lasers. These include the development of computer programs that use boundary layer approximations in the mixing region,¹⁻³ an "exact" analytical flame-sheet solution for laminar mixing in the limit of zero power⁴ or optical saturation,⁵ and solutions in which simplified mixing and chemical kinetics models are used.^{6,7} The latter do not satisfy the equations of motion, even in a limiting sense, but do describe the basic behavior of the cw diffusion-type chemical laser in terms of relevant normalized parameters.

A flame-sheet diffusion model was used by Mirels, Hofland, and King.⁶ Laminar and turbulent mixing were analyzed as well as oscillator and amplifier configurations. In order to obtain simple closed-form solutions, a two-level vibrational model was used.

Broadwell⁷ extended the analysis of Emanuel and Whittier⁸ to include effects of diffusion on HF laser performance. A scheduled-mixing model was used; turbulent mixing and an oscillator optical configuration were assumed; multiple vibrational levels were considered.

In the present study, the analysis of Mirels, Hofland, and King⁶ is extended to include multiple vibrational levels. Arbitrary mixing rates and chemical rate coefficients are considered. Solutions for zero power and amplifier cases, as well as expressions for total oscillator output power, are obtained. In addition, the flame-sheet⁶ and the scheduled-mixing⁷ models

are compared. The formulation presented herein can be used for any diffusion-type chemical laser. Both cold-reaction, e.g., $\text{H}_2 + \text{F} \rightarrow \text{HF}(\text{v}) + \text{H}$, and chain-reaction, e.g., $\text{H}_2 + \text{F} \rightarrow \text{HF}(\text{v}) + \text{H}$, $\text{H} + \text{F}_2 \rightarrow \text{HF}(\text{v}) + \text{F}$ HF lasers are considered. These developments go beyond the treatment of Broadwell⁷ in that he assumed a cold reaction HF laser, turbulent mixing, and particular numerical values for chemical rate coefficients.

II. THEORY

In the following sections, the rate of formation and deactivation of excited species in a cw diffusion-type chemical laser is discussed. Equations that describe the performance of amplifier or oscillator configurations are then noted. In order to fix the ideas, a cold-reaction HF(DF) laser is considered in Sections II and III. The extension to a chain-reaction HF(DF) laser is noted in Appendix A.

A. BASIC EQUATIONS

The mixing model of Mirels, Hofland, and King⁶ is illustrated in Fig. 1. The flow downstream of a single oxidizer (F) semichannel is considered. The reactants are assumed to be premixed, but do not start to react until a specified flame sheet location is reached. The effect of diffusion is accounted for by the flame sheet shape. The flame sheet ordinates (x_o , y_f) are given by

$$y_f = y_f(x_o) \quad x_o \leq x_D \quad (1a)$$

$$= w \quad x_o > x_D \quad (1b)$$

where w is the width of the semichannel, and x_D is the axial distance required for the flame sheet to reach the channel centerline. Flow velocity, pressure, and temperature are assumed to remain constant. The semichannel is assumed to have a unit height.

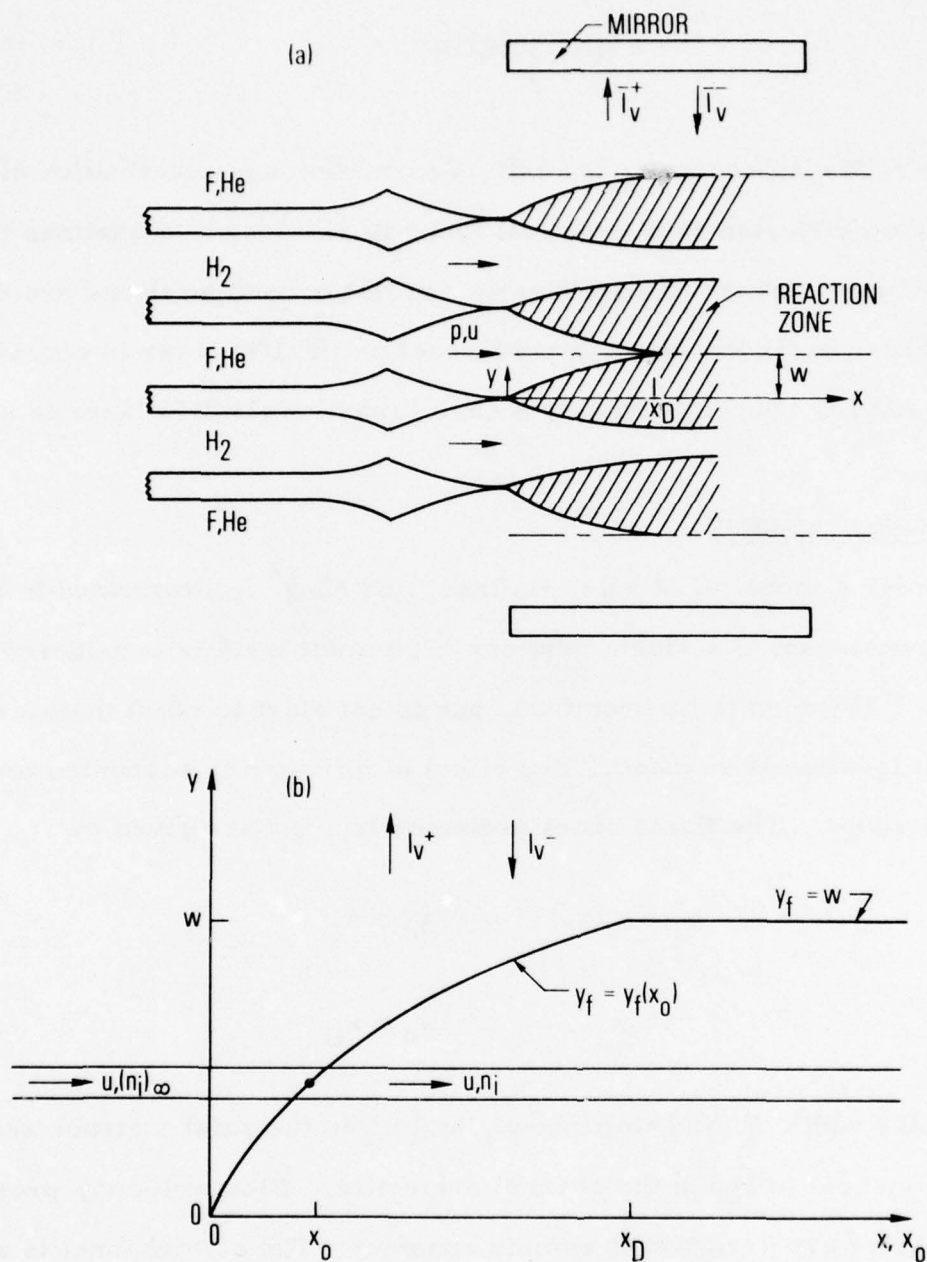


Figure 1. Mixing Model of Mirels, Hofland, and King. Reactants are premixed. Reaction starts at x_0 , i. e., at intercept of stream tube with flame sheet $y_f = y_f(x_0)$. $\bar{I}_V = \bar{I}_V^+ + \bar{I}_V^-$. (a) Typical physical flow; (b) Corresponding model semi-channel flow.

Let n_v denote the number density (mole/cm³) of molecules at vibrational level v . Vibrational levels from $v = 0$ to $v = v_f$ are considered. The molecules in each vibrational level are assumed to be in rotational equilibrium at a temperature equal to the local translational temperature T . Only P-branch transitions ($v + 1, J - 1 \rightarrow v, J$) are considered. The gain associated with these transitions can be expressed as

$$g_{v,J} = \sigma_{v,J}(n_{v+1} - A_{v,J}n_v) \quad (2a)$$

where

$$A_{v,J} = e^{-2JT_R/T} \quad (2b)$$

The value of $\sigma_{v,J}$ at line center of a Doppler-broadened P-branch transition can be found from⁸

$$\sigma_{v,J} = 3.29 \times 10^{47} \bar{\sigma} T_R M^{1/2} T^{-3/2} M_{v,J}^2 e^{-J(J-1)T_R/T} \quad (2c)$$

where, for an HF lasing molecule, $\bar{\sigma} = 1$, $T_R = 30.16$ K, $M = 20$ g/mole,

$$M_{o,J}^2 \times 10^{38} = 0.96 [1 + 0.063J] \text{ erg-cm}^3 \quad (2d)$$

$$M_{v,J}^2 / M_{o,J}^2 = 1 + v - 0.01 v^3 \quad (2e)$$

$$\sigma_{o,1} = 5.66 \times 10^7 (400/T)^{3/2} \text{ cm}^2/\text{mole} \quad (2f)$$

Equations (2d) and (2e) are correlations of estimates provided by Herbelin that are believed to be accurate to within about 10% for $1 \leq J \leq 16$ and $v \leq 6$.

For convenience, the symbols $g_{v,J}$, $\sigma_{v,J}$, and $A_{v,J}$ are now denoted g_v , σ_v , and A_v , respectively; i. e., the dependence on J is not displayed. It is assumed that, when lasing occurs, only one transition, with intensity denoted by $\bar{I}_{v,J} \equiv \bar{I}_v$, is permitted between $v+1$ and v . In order to obtain closed-form solutions, vibration-vibration ($v-v$) collisions are neglected. The rate of change of n_v in each stream tube can then be expressed as

$$\begin{aligned} \frac{dn_v}{dx} = & u \left(\frac{dn_v}{dx} \right)_p + \left[\left(k_{cd}^{(v+1)} + k_{sp}^{(v+1)} \right) n_{v+1} - \left(k_{cd}^{(v)} + k_{sp}^{(v)} \right) n_v \right] \\ & + \left[\left(\frac{\bar{I}_v}{\epsilon} \right)_v - \left(\frac{\bar{I}_v}{\epsilon} \right)_{v-1} \right] \end{aligned} \quad (3)$$

where $u(dn_v/dx)_p$ is the rate (mole/cm³/sec) of formation of n_v by the chemical "pumping" reaction, as discussed in Appendix A. The second term on the right side of Eq. (3) is the net rate of formation of n_v by collisional deactivation (see Appendix A) and by spontaneous emission. The quantities $k_{cd}^{(v)}$ and $k_{sp}^{(v)}$ are the rates (sec⁻¹) of collisional deactivation and spontaneous emission, respectively, from v to $v-1$ levels. Note that $k_{sp}^{(0)} = k_{cd}^{(0)} = 0$. Generally, $k_{sp}^{(v)}/k_{cd}^{(v)} \ll 1$ for HF lasers. The last term on the right side of Eq. (3) is the net rate of formation of n_v due to stimulated emission.

We now introduce the following normalized variables

$$\begin{aligned}
 \zeta &= x k_{cd}^{(1)} / u & I_v &= \sigma_v \bar{I}_v / \left(\epsilon_v k_{cd}^{(1)} \right) \\
 N_i &= (n_r w)^{-1} \int_0^{y_i} n_i dy & G_v &= (\sigma_v n_r w)^{-1} \int_0^{y_f} g_v dy \\
 r_v &= \left(k_{cd}^{(v)} + k_{sp}^{(v)} \right) / k_{cd}^{(1)} & &= N_{v+1} - A_v N_v
 \end{aligned} \tag{4}$$

The quantity n_r is a reference number density, which, for a cold-reaction HF laser, is taken to equal $(n_F)_\infty$. Equation (3) is integrated with respect to y , between the limits $y = 0$ and $y = y_f$. If it is assumed that r_v is a constant, I_v is a function only of x , i.e., a mean value is used at each station, and $n_v = 0$ at the flame sheet, the result is

$$\begin{aligned}
 dN_v/d\zeta + (r_v + I_{v-1} + A_v I_v) N_v - (r_{v+1} + I_v) N_{v+1} - (A_v N)_{v-1} \\
 = (dN_v/d\zeta)_p
 \end{aligned} \tag{5a}$$

with the boundary condition $N_v(0) = 0$. An alternative form of Eq. (5a) that retains G_v is

$$dN_v/d\zeta - (r_{v+1} N_{v+1} - r_v N_v) - (I_v G_v - I_{v-1} G_{v-1}) = (dN_v/d\zeta)_p \tag{5b}$$

Let $N_{\text{ToT}} = \sum_{v=0}^{v_f} N_v$. Since N_{ToT} can be changed only by the pumping process, it follows that

$$dN_{\text{ToT}}/d\zeta = \sum_{v=0}^{v_f} (dN_v/d\zeta)_p \quad (5c)$$

For a cold-reaction HF laser, Eq. (A-5),

$$(dN_v/d\zeta)_p = a_v K_1 N_F \quad (6a)$$

where

$$K_1 N_F = K_1 e^{-K_1 \zeta} \int_0^{\zeta} e^{K_1 \zeta_0} \frac{dY_0}{d\zeta_0} d\zeta_0 \quad (6b)$$

$$= dY/d\zeta \quad (K_1 \rightarrow \infty) \quad (6c)$$

Here $Y_0 = y_f(x_0)/w$, $Y = y_f(x)/w$, $k_p = \sum_{v=0}^{v_f} k_p^{(v)}$, $a_v = k_p^{(v)}/k_p$, $K_1 = k_p/k_{cd}^{(1)}$, and $n_r = (n_F)_\infty$. The rate of change of the total N_v population is, from Eqs. (5c) and (6a)

$$dN_{\text{ToT}}/d\zeta = K_1 N_F \quad (7)$$

Conservation of F atoms yields

$$N_{\text{ToT}} + N_F = Y \quad (8)$$

It follows that

$$N_{ToT} = K_1 e^{-K_1 \zeta} \int_0^{\zeta} e^{K_1 \zeta_o} Y_o d\zeta_o \quad (9a)$$

$$= Y \quad (K_1 \rightarrow \infty) \quad (9b)$$

The flame sheet shape can be expressed in the form

$$Y = (\zeta / \zeta_D)^m \quad Y_o = (\zeta_o / \zeta_D)^m \quad (\zeta \leq \zeta_D) \quad (10a)$$

$$Y = 1 \quad Y_o = 1 \quad (\zeta > \zeta_D) \quad (10b)$$

where $m = 1/2$ and 1 for laminar and turbulent mixing, respectively.

Now let ϕ_v denote the number of photons emitted up to station ζ , per initial n_r particle, from the transition $v + 1, J - 1 \rightarrow v, J$. Thus

$$\phi_v = (un_r w)^{-1} \int_0^x dx \int_0^{y_f(x)} (g\bar{I}/\epsilon)_v dy \quad (11)$$

$$= \int_0^{\zeta} I_v G_v d\zeta \quad (12)$$

The quantity $d\phi_v/d\zeta = I_v G_v$ is a measure of the local emitted photon flux per initial n_r particle. Let P denote the net output power, per semichannel, up to station ζ . It follows that

$$P = un_r w \sum_{v=0}^{v_f-1} \epsilon_v \phi_v \quad (13)$$

When a mean photon energy ϵ is used, $P = un_r w \epsilon \phi$, where $\phi \equiv \sum_{v=0}^{v_f-1} \phi_v$ is the net photon output per initial n_r particle up to station ζ .

B. ZERO-POWER AND AMPLIFIER CASES

When I_v is specified, Eq. (5a) is linear and generally can be integrated in closed form in order to find N_v as a function of ζ . The net gain per semichannel is then found from $G_v = N_{v+1} - (AN)_v$.

For the zero-power case ($I_v = 0$), Eq. (5a) yields

$$N_v e^{r_v \zeta} = a_v K_1 \int_0^{\zeta} e^{r_v \zeta} N_F d\zeta + r_{v+1} \int_0^{\zeta} e^{r_v \zeta} N_{v+1} d\zeta \quad (14)$$

Equation (14) is integrated successively, starting with $v = v_f$. Note that $r_0 = 0$. Expressions for N_v and G_v are given in Appendix B.

It is of interest to expand Eq. (5a) in a power series about $\zeta = 0$. Consider the case $K_1 \rightarrow \infty$, $Y = (\zeta/\zeta_D)^m$. It is found that

$$N_v/Y = a_v + \zeta(m+1)^{-1}[(r_{v+1} + I_v)a_{v+1} + (A I a)_{v-1} - (r_v + I_{v-1} + A_v I_v)a_v] \zeta=0 + O(\zeta^2) \quad (15a)$$

For the zero-power case

$$N_v/Y = a_v + \zeta(m+1)^{-1}[(ra)_{v+1} - (ra)_v] + O(\zeta^2) \quad (15b)$$

The corresponding gain per semichannel is

$$G_v/Y = (a_{v+1} - A_v a_v) + \zeta(m+1)^{-1} \left\{ [(ra)_{v+2} - (ra)_{v+1}] - A_v [(ra)_{v+1} - (ra)_v] \right\} + O(\zeta^2) \quad (15c)$$

The first term on the right side of Eqs. (15) is the contribution of the pumping reaction, and the second term is the modification because of radiative and collisional deactivation. The pumping reaction increases N_v and G_v by an amount proportional to Y , whereas deactivation increases (or decreases) N_v and G_v by an amount proportional to ζY . Equations (15) are similar in form to the results of Hofland and Mirels,^{4,5} where a laminar flame-sheet solution was obtained by expansion about $x = 0$.

Zero-power number density and gain distributions for a cold-reaction HF laser, in the limit $K_1 \rightarrow \infty$, $Y = (\zeta/\zeta_D)^m$, are given in Fig. 2. For

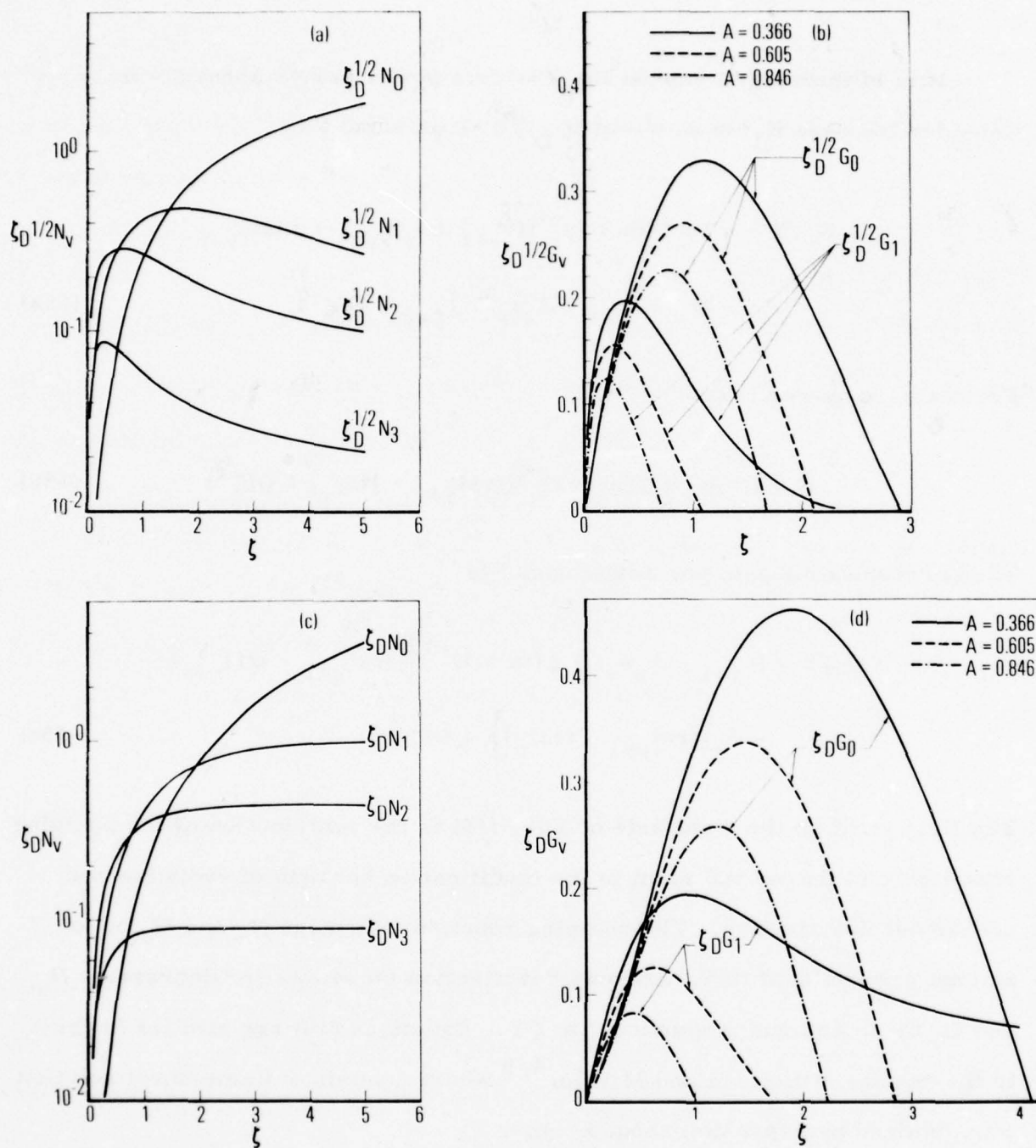


Figure 2. Zero-Power Number Density and Gain Distribution for Cold-Reaction HF Laser. $K_1 \rightarrow \infty$, $Y = (\zeta/\zeta_D)^m$, $r_v = v$, $v_f = 3$, $a_v = 0.0, 0.17, 0.55, 0.28$. (a) Number density, $m = 1/2$; (b) Gain, $m = 1/2$; (c) Number density, $m = 1$; (d) Gain, $m = 1$.

small ζ , N_v and G_v vary as Y . In the limit $\zeta \rightarrow \infty$, $N_0 \rightarrow Y$, and for $v \neq 0$, $N_v \sim \zeta^{m-1}$. The population inversion is total for small ζ and becomes partial with increases in ζ . The gain per semichannel is a maximum at values of ζ of order 1. In interpreting Figs. 2b and 2d, it should be recalled that, in physical variables, the gain per semichannel is proportional to $\sigma_v G_v \sim (v+1)G_v$ for a fixed value of J . Hence, for laminar flow and fixed J , the peak gain on the 2-1 transition is somewhat larger than the peak gain on the corresponding 1-0 transition (Fig. 2b), although this is not true for turbulent flow (Fig. 2d).

The present results are expected to be modified somewhat by vibration-vibration collisions, which are neglected herein. These results are useful however, for providing convenient first estimates of zero-power number density and gain.

C. OSCILLATOR CASES

We now estimate net oscillator output power following a procedure similar to that used by Broadwell⁷ and Emanuel and Whittier.⁸ A Fabry-Perot optical cavity is assumed. Steady-state lasing is assumed to be initiated simultaneously on all transitions ($v = 0, 1, 2, \dots, v_f-1$) at some station denoted ζ_i . The value of J is assumed to be the same for each lasing transition, i.e., $A_v = A = \text{const.}$ The choice for J is discussed later. All photons are assumed to have the same energy, i.e., $\epsilon_v = \epsilon$.

The condition for steady-state lasing requires that, in the lasing region,⁸

$$\begin{aligned} \sigma_v G_v &= [(-1) \ln(R_1 R_2)] / [2n_{sc} n_r w] & v < v_f \\ &\equiv \sigma_0 G_c & \end{aligned} \quad (16)$$

where R_1 and R_2 are the cavity mirror reflectivities, and n_{sc} is the number of semichannels between the mirrors. The quantity $G_c = \sigma_v G_v / \sigma_o$ denotes the constant value of G_o in the lasing region. Equation (16) does not apply at $v = v_f$ because there is no lasing from $v_f + 1 \rightarrow v_f$. For a given optical cavity, laser geometry, and flow conditions, the product $\sigma_o G_c$ is a constant. However, the individual values of σ_o and G_c depend on the choice for J . Saturated laser operation corresponds to $G_c \rightarrow 0$.

Upstream of ζ_i , $\phi = 0$. The variation of ϕ with ζ , downstream of ζ_i , is found as follows. Equation (5b) can be expressed as

$$I_v G_v = dN_v/d\zeta - (dN_v/d\zeta)_p + r_v N_v - r_{v+1} N_{v+1} + I_{v-1} G_{v-1} \quad (17)$$

Successive solutions of Eq. (17) for $I_o G_o$, $I_1 G_1$, etc., yield

$$I_v G_v = \sum_{i=0}^v [dN_i/d\zeta - (dN_i/d\zeta)_p] - r_{v+1} N_{v+1} \quad (18)$$

The rate of change of net photon output is, then, after algebraic simplification

$$\begin{aligned} d\phi/d\zeta &\equiv \sum_{v=0}^{v_f-1} I_v G_v \\ &= \sum_{v=0}^{v_f} [v(a_v dN_{ToT}/d\zeta - dN_v/d\zeta) - r_v N_v] \end{aligned} \quad (19)$$

Equation (19) can be deduced more directly by consideration of conservation of vibrational energy; i.e., the rate of change of output power equals the rate of increase of vibrational energy created by the pumping process less the rate of increase of vibrational energy of the N_v particles, less the rate of energy lost by vibration-translation collisions. It is clear that vibration-vibration collisions conserve vibrational energy, and if these had been included in the present study they would not appear in Eq. (19).

We now express N_v in terms of G_o and N_{ToT} , which are known quantities. Successive solutions of $N_v = G_{v-1} + AN_{v-1}$ for N_1, N_2 , etc., indicate

$$N_v = A^{v-1} \sum_{i=0}^{v-1} (G_i / A^i) + A^v N_o \quad (20)$$

where the summation is taken equal to zero for $v = 0$. An expression for N_o is found by summing Eq. (20) for $v = 0, 1, \dots, v_f$. The result is

$$N_o \sum_{o=0}^{v_f} A^v = N_{ToT} - \sum_{v=0}^{v_f-1} G_v \sum_{i=0}^{v_f-1-v} A^i \quad (21)$$

Substitution of Eq. (21) into Eq. (20) yields

$$N_v = F_v N_{ToT} + H_v G_c \quad (22)$$

where

$$F_v = A^v / \sum_{v=0}^{v_f} A^v \quad (23a)$$

$$H_v = A^{v-1} \sum_{i=0}^{v-1} \frac{\sigma_o/\sigma_i}{A^i} - F_v \sum_{v=0}^{v_f-1} (\sigma_o/\sigma_v) \sum_{i=0}^{v_f-1-v} A^i \quad (23b)$$

Equation (23a) can be expressed as

$$\begin{aligned} F_v &= A^v (A - 1) / (A^{v_f+1} - 1) & A \neq 1 \\ &= (v_f + 1)^{-1} & A = 1 \end{aligned} \quad (24a)$$

For $\sigma_o/\sigma_v = 1$, Eq. (23b) becomes

$$\begin{aligned} H_v &= [A^v (1 + v_f) / (A^{v_f+1} - 1)] - (A - 1)^{-1} & A \neq 1 \\ &= v - (v_f/2) & A = 1 \end{aligned} \quad (24b)$$

The quantities F_v and H_v are independent of ζ . Also, $\sum_{v=0}^{v_f} F_v = 1$, $\sum_{v=0}^{v_f} H_v = 0$. Thus, N_v is known. Substitution of Eq. (22) into Eq. (19) yields

$$d\phi/d\zeta = C_1 dN_{ToT}/d\zeta - C_2 N_{ToT} - C_3 G_c \quad (25a)$$

where it is assumed that $dG_c/d\zeta = 0$.

where

$$C_1 = \sum_{v=1}^{v_f} v(a_v - F_v)$$

$$C_2 = \sum_{v=1}^{v_f} r_v F_v$$

$$C_3 = \sum_{v=1}^{v_f} r_v H_v$$

If terms of order A compared with one are neglected, $C_1 = \sum_{v=1}^{v_f} v a_v$, $C_2 = A$, $C_3 = \sum_{v=1}^{v_f} r_v (\sigma_0 / \sigma_{v-1})$. The latter equals v_f when $r_v = \sigma_{v-1} / \sigma_0 = v$. From the definition of C_1 , it is clear that C_1 equals the number of photons liberated per lasing species molecule (formed by the chemical reaction) for the case of a saturated laser with no collisional deactivation. Similarly, C_2 is the ratio of the net collisional deactivation rate in a saturated laser to the collisional deactivation rate that would exist if all the lasing species molecules were in the first vibrational level. The quantity $C_3 G_c / N_{ToT}$ is the correction to C_2 , i.e., increased collisional deactivation, due to a lack of optical saturation.

Equation (25a) applies downstream of ζ_i . The net photon output, up to station ζ , is

$$\phi = C_1 [N_{ToT}]_{\zeta_i}^{\zeta} - C_2 \int_{\zeta_i}^{\zeta} N_{ToT} d\zeta - C_3 G_c (\zeta - \zeta_i) \quad (25b)$$

The optical cavity is assumed to end at the streamwise station, where $d\phi/d\zeta$ becomes zero or negative. The latter station is denoted ζ_e , and the corresponding net photon output and power output are denoted ϕ_e and P_e , respectively. If ΔH represents the chemical energy released, per mole of n_r particles, the chemical efficiency of the laser is

$$\eta_c \equiv P_e / (n_r u w \Delta H) = (\epsilon / \Delta H) \phi_e \quad (26)$$

where $\epsilon / \Delta H = 1/3$ for a cold-reaction HF laser operating at 2.706 μm . The product $2.327 \phi_e$ yields the output at this wavelength in terms of kilojoules per gram of fluorine.

Oscillator performance can now be deduced. Consider the limit $K_1 \rightarrow \infty$ with a flame sheet given by $Y = (\zeta / \zeta_D)^m$ for $\zeta < \zeta_D$, and $Y = 1$ for $\zeta > \zeta_D$. Equations (25) yield

$$\zeta_D^m (d\phi/d\zeta) = m C_1 \zeta^{m-1} - C_2 \zeta^m - C_3 \zeta_D^m G_c \quad (\zeta_i < \zeta < \zeta_D) \quad (27a)$$

$$\frac{\phi_e}{C_1} = \left\{ \left(\frac{\zeta}{\zeta_D} \right)^m - \frac{C_2 \zeta_D}{(m+1) C_1} \left(\frac{\zeta}{\zeta_D} \right)^{m+1} - \left(\frac{C_3 G_c}{C_2} \right) \left(\frac{C_2 \zeta}{C_1} \right) \right\}_{\zeta=\zeta_i}^{\zeta=\zeta_e} \quad (27b)$$

where, for $(C_2 \zeta_D / m C_1) \geq [1 + (C_3 G_c / C_2)]^{-1}$

$$\left(\frac{C_2 \zeta_e}{m C_1} \right)^m = \left[1 + \frac{C_2 \zeta_D}{2 C_1} \left(\frac{C_3 G_c}{C_2} \right)^2 \right]^{1/2} - \left(\frac{C_2 \zeta_D}{2 C_1} \right)^{1/2} \frac{C_3 G_c}{C_2} \quad (m = 1/2) \quad (28a)$$

$$= 1 - \frac{C_2 \zeta_D}{C_1} \frac{C_3 G_c}{C_2} \quad (m = 1) \quad (28b)$$

and for $(C_2 \zeta_D / m C_1) \leq [1 + (C_3 G_c / C_2)]^{-1}$

$$\zeta_e = \zeta_D \quad (28c)$$

Equations (28a) and (28b) are obtained by setting Eq. (27a) equal to zero, and correspond to cases where lasing terminates before the flame sheet reaches the channel centerline. Equation (28c) corresponds to cases where lasing is terminated when the flame sheet reaches the channel centerline. The quantity ζ_i can be found from Eq. (16) and the equations given in Appendix B. In most cases, $\zeta_i^2 \ll 1$, and Eq. (15c) can be expressed

$$\left(\frac{\zeta_i}{\zeta_D} \right)^m = \frac{\sigma_o G_c}{\sigma_v (a_{v+1} - A a_v)} \left[1 - \frac{\zeta_i}{m+1} \frac{[(ra)_{v+1} - (ra)_{v+2}] - A [(ra)_v - (ra)_{v+1}]}{a_{v+1} - A a_v} + o(\zeta_i^2) \right]^{-1} \quad (29)$$

where $\sigma_0 G_c$ is given by Eq. (16). Equation (29) is written in a form that can be solved for ζ_i by iteration with $\zeta_i = 0$ used as the initial estimate. For a given value of J , the value of v that yields the smallest value of ζ_i ; i.e., corresponds to the transition with the largest zero power gain, is used. The choice of $v = 1$ (2) appears appropriate for cold-reaction HF(DF) lasers. If no solution for ζ_i is obtained, threshold is not reached.

In most practical devices, the optical medium is saturated, and lasing originates near $\zeta = 0$. In these cases, Eqs. (27) and (28) can be considerably simplified. Assume that $(\zeta_i/\zeta_D)^m \equiv 0(G_c) \ll 1$, $(C_3 G_c/C_2)^2 \ll 1$, and $C_2 \zeta_D/C_1 = 0(1)$. Equations (27) and (28) become, for $C_2 \zeta_D/mC_1 \geq [1 + (C_3 G_c/C_2)]^{-1}$

$$(m+1) \left(\frac{C_2 \zeta_D}{mC_1} \right)^m \frac{\phi_c}{C_1} = 1 - m(m+1) \left(\frac{C_2 \zeta_D}{mC_1} \right)^m \frac{C_3 G_c}{C_2} + O(G_c) + O[(C_3 G_c/C_2)^2] \quad (30a)$$

$$\left(\frac{C_2 \zeta_e}{mC_1} \right)^m = 1 - \left(\frac{mC_2 \zeta_D}{C_1} \right)^m \frac{C_3 G_c}{C_2} + O \left(\frac{C_3 G_c}{C_2} \right)^{2(1-m)/m} \quad (30b)$$

and for $C_2 \zeta_D/mC_1 \leq [1 + (C_3 G_c/C_2)]^{-1}$

$$\frac{\phi_e}{C_1} = 1 - \left(\frac{1}{m+1} + \frac{C_3 G_c}{C_2} \right) \frac{C_2 \zeta_D}{C_1} + O(G_c) \quad (30c)$$

$$\zeta_e = \zeta_D \quad (30d)$$

Equations (30) are plotted in Fig. 3 for $m = 1/2$ and define saturated laser performance.

Values of C_1 , C_2 , and C_3 are given in Table 1 as a function of A for values of a_v , r_v , σ_v/σ_o , and v_f appropriate for a cold-reaction HF laser. For this case,

$$C_1 = 2.11 - C_2 \quad (31a)$$

$$C_2 = A(1 - A)(1 + 2A + 3A^2)/(1 - A^4) \quad (31b)$$

and, to within 1%, $C_3 = 3.0 + 1.7 A(1 - A)$. It is seen that $C_2 \rightarrow 0$ as $A \rightarrow 0$. This result is explained as follows. Recall that C_2 is the ratio of the collisional deactivation rate in a saturated laser to the collisional deactivation rate that would exist if all the lasing species molecules, i.e., HF, were in the first vibrational level. When $A = 0$ in a saturated laser, stimulated emission reduces all lasing molecules to the ground state. Hence, there is no collisional deactivation in this case, and $C_2 = 0$. This limit can not be achieved in practice because $\sigma_o \rightarrow 0$ as $A \rightarrow 0$ such that $G_c \equiv (\sigma_o G_c)/\sigma_o \rightarrow \infty$ for nonzero values of $\sigma_o G_c$.

We have assumed that the value of J is the same for all lasing transitions, but the choice for J has not yet been established. In Fig. 4 is indicated the effect of J on HF laser output for the realistic range of conditions $0 \leq \sigma_o G_c \leq 10^5 \text{ cm}^2/\text{mole}$, $0.0 \leq \zeta_D \leq 20$, and $T = 300 \text{ K}$ and 600 K . For these conditions and small values of J , the optical medium is saturated, and laser output

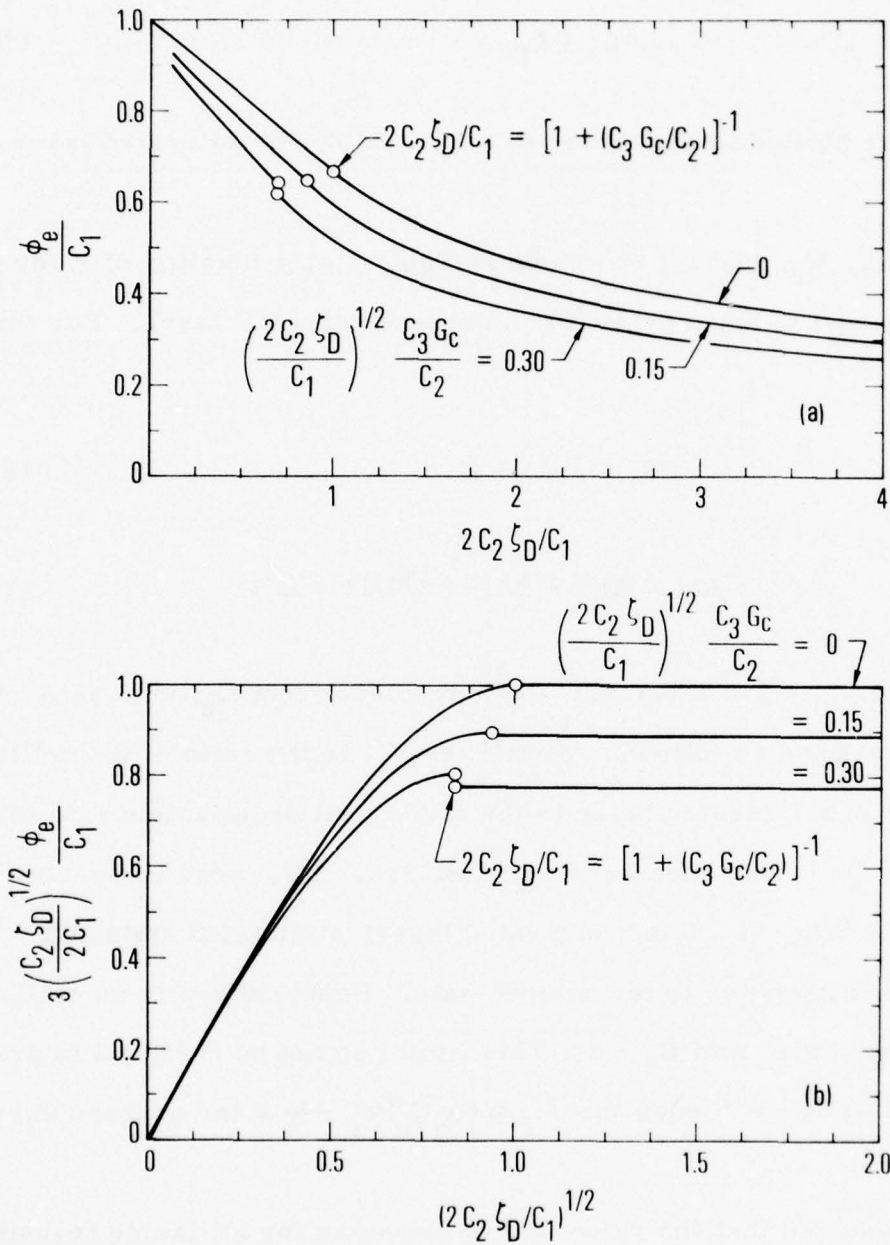


Figure 3. Saturated Laser Performance for $K_1 \rightarrow \infty$ and $m = 1/2$, [Eqs. (30)]. (a) Efficiency; (b) Output power.

Table 1. Parameters for Defining Oscillator Performance
for Cold-Reaction HF Lasers^a

A	$\frac{JT_R}{T}$	C ₁	C ₂	C ₃
0.00	∞	2.110	0.000	3.000
0.10	1.151	1.999	1.107 (-1)	3.159
0.20	8.047 (-1)	1.866	2.436 (-1)	3.291
0.30	6.020 (-1)	1.714	3.959 (-1)	3.380
0.40	4.581 (-1)	1.548	5.616 (-1)	3.424
0.50	3.466 (-1)	1.377	7.333 (-1)	3.422
0.60	2.554 (-1)	1.206	9.044 (-1)	3.382
0.70	1.783 (-1)	1.041	1.069	3.312
0.80	1.116 (-1)	8.851 (-1)	1.225	3.220
0.90	5.268 (-2)	7.413 (-1)	1.369	3.114
1.00	0.000	6.100 (-1)	1.500	3.000

^a $r_v = v$; $v_f = 3$; $\sigma_v/\sigma_o = 1 + v$; $a_o, a_1, a_2, a_3 = 0.00, 0.17, 0.55, 0.28$.

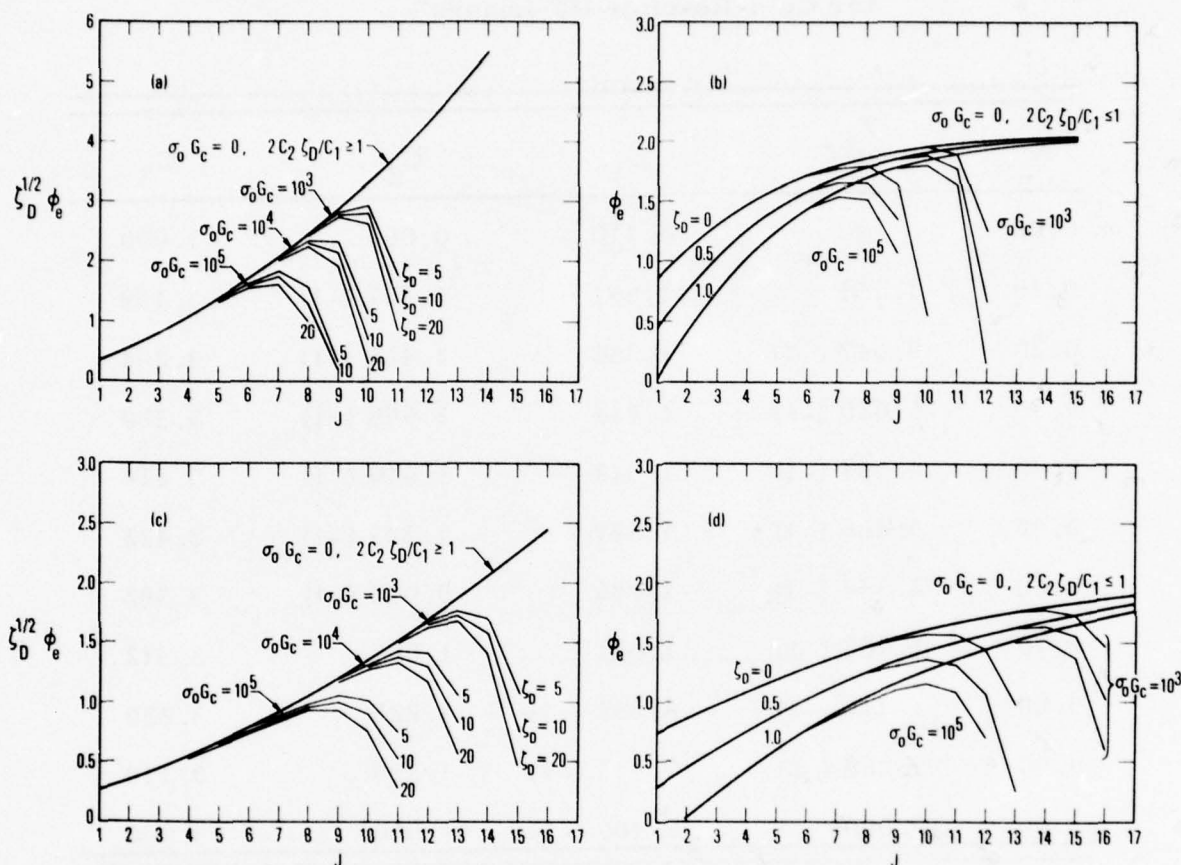


Figure 4. Effect of J Variation on Output Power from Cold-Reaction HF Chemical Laser. $K_1 \rightarrow \infty$, $m = 1/2$, $r_v = v$, $\sigma_v/\sigma_0 = v + 1$, $a_v = 0.0, 0.17, 0.55, 0.28$, $\sigma_0 G_c = \text{cm}^2/\text{mole}$. (a) $T = 300 \text{ K}$, $5 \leq \zeta_D \leq 20$; (b) $T = 300 \text{ K}$, $0 \leq \zeta_D \leq 1$; (c) $T = 600 \text{ K}$, $5 \leq \zeta_D \leq 20$; (d) $T = 600 \text{ K}$, $0 \leq \zeta_D \leq 1$.

increases with increase in J . With further increase in J , the medium becomes unsaturated because of the decrease in σ_v with increase in J , i.e., Eqs. (2c) and (2f), and laser output reaches a maximum.[†] Thereafter, an increase in J results in reduced laser output. Further increases in J result in threshold not being reached. Emanuel and Whittier⁸ recommended that the value of J that yields the maximum output power be used to estimate laser performance. This approach may tend to overestimate J and laser output power because lasing at each streamwise station actually occurs on those transitions with the highest gain – and these transitions appear to be at somewhat lower values of J than those that yield the highest output power. The method of Emanuel and Whittier⁸ thus provides an upper bound on laser performance. An alternative approach is to use values of J that are observed experimentally. In typical cold-reaction HF and DF lasers, the output power appears to be centered about $J = 5$ to 8 and $J = 8$ to 10 transitions, respectively,^{9, 10} although these results depend somewhat on initial gas temperatures and the degree of dilution. Hence, the values $J = 7, 9$ appear to be representative experimental values for HF and DF lasers, respectively. Further study concerning the choice for J is desirable.

[†]The maxima in Fig. 4 are predicted to within a few percent by using $\zeta_i = 0$ in Eq. (27b).

III. DISCUSSION OF RESULTS

The dependent variables are functions of the independent variable ζ ; the parameters ζ_D , K_1 , G_c , A , J (or T), and m ; and lasing molecule distributive properties (r_v , σ_v/σ_o , a_v). The quantities ζ , ζ_D , and K_1 are the ratios of streamwise distance, characteristic diffusion distance, and characteristic pumping distance to characteristic collisional deactivation distance, whereas the quantity G_c is a measure of optical saturation. For zero-power cases with $\zeta \leq \zeta_D$, the dependent variables $\zeta_D^m N_v$, $\zeta_D^m G_v$ are independent of ζ_D . In oscillator cases, the quantities ϕ_e/C_1 and $C_2 \zeta_e/C_1$ depend on $C_2 \zeta_D/C_1$, $C_3 G_c/C_2$, $C_1 K_1/C_2$, and $C_2 \zeta_i/C_1$. When $\zeta_i^2 \ll 1$ and $C_2 \zeta_D/C_1 \geq [1 + (C_3 G_c/C_2)]^{-1}$, the quantity $(C_2 \zeta_D/C_1)^m \phi_e/C_1$ is a function only of $(C_2 \zeta_D/C_1)^m (C_3 G_c/C_2)$ and $C_1 K_1/C_2$.

In practical lasers, the assumptions incorporated in Eq. (30) are approximately valid. The resulting variation of efficiency and output power with $C_2 \zeta_D/m C_1$ and $(C_2 \zeta_D/m C_1)^{1/2} (C_3 G_c/C_2)$ is shown in Fig. 3 for $m = 1/2$. Note that $(C_2 \zeta_D/m C_1)^{1/2} (C_3 G_c/C_2)$ is independent of pw. For small values of ζ_D , the flow corresponds to that for a premixed laser. In Fig. 3a, it is indicated that laser efficiency decreases as ζ_D increases. The ordinate in Fig. 3b is proportional to output power per semichannel when plenum temperatures and a stoichiometry (p_F/p) are kept constant. It is shown that output power increases with ζ_D until $C_2 \zeta_D/m C_1 = [1 + (C_3 G_c/C_2)]^{-1}$ and remains constant with further increases in ζ_D . In the latter region, lasing is terminated before the fuel (H_2) reaches the centerline of the oxidizer (F) channel.

The present results can readily be expressed in terms of physical variables. We first consider a cold-reaction HF laser with combustor-generated DF present in the oxidizer flow. Let p_F and p_{DF} denote the initial partial pressures of atomic fluorine and DF, respectively, and let p_F characterize the mean value of p_{HF} in the reaction zone. We assume that HF and DF are the major deactivators of HF(v) and use only the leading terms in Eqs. (A-18) and (A-19). Recall that $\zeta = k_{cd}^{(1)} x/u$. It follows that

$$\zeta = \frac{0.0752 p(\text{torr})x(\text{cm})}{(p/p_F)(T/400)^2} \left(\frac{4 \times 10^5}{u} \right) [1 + 0.6 (p_{DF}/p_F)] \quad (32)$$

Characterize laminar and turbulent flame shapes by $y_D^L = A_L (\mathcal{D}x/u)^{1/2}$ and $y_f^T = A_T x$, respectively, where $A_L = 0(1)$, $A_T = 0(0.1)$, and $\mathcal{D} = CT^{3/2}/p$ is the laminar diffusion coefficient. Then, $x_D^L = (w/A_L)^2 u/\mathcal{D}$, $x_D^T = w/A_T$, and the corresponding laminar and turbulent values of ζ_D^m are

$$(\zeta_D^L)^{1/2} = \frac{2.072 p(\text{torr})w(\text{cm})}{(p/p_F)^{1/2}(T/400)^{7/4}} \left(\frac{2.88 \times 10^{-4}}{C} \right)^{1/2} \left(\frac{2}{A_L} \right) [1 + 0.6 (p_{DF}/p_F)]^{1/2} \quad (33a)$$

where $C = 2.88 \times 10^{-4}$ corresponds to the diffusion of H_2 into He and

$$\zeta_D^T = \frac{0.752 p(\text{torr})w(\text{cm})}{(p/p_F)(T/400)^2} \frac{4 \times 10^5}{u} \frac{0.1}{A_T} [1 + 0.6 (p_{DF}/p_F)] \quad (33b)$$

Similarly, if we let $\sigma_o = \sigma_{o,J}$ and $n_r = p_F/RT$, Eq. (16) becomes, for a HF lasing molecule,

$$G_c = \frac{0.234 (p/p_F)(T/400)^{5/2} \ln(R_1 R_2)^{-1}}{n_{sc} p(\text{torr})w(\text{cm})} \frac{\exp[J(J-1)T_R/T]}{J(1 + 0.063 J)} \quad (33c)$$

where $\sigma_{o,J}$ has been evaluated from Eqs. (2). Note that $\zeta_D^m G_c$ is independent of pw. Recall that $C_1 = 2.11$, $C_3 = 3$, and $C_2 = \exp(-2JT_R/T)$ for a HF laser with $C_2 \ll 1$. Hence, the dependence of laser performance on physical variables can be readily deduced, e.g., Fig. 3 and Eqs. (33).

We now note explicit expressions for ϕ_e and ζ_e for a saturated laser ($G_c = 0$) in the limit $K_1 \rightarrow \infty$, $C_2 \zeta_D/mC_1 > 1$. From Eqs. (30) and (33)

$$\phi_e = 0.228 \frac{C_1^{3/2}}{C_2^{1/2}} \frac{(p/p_F)^{1/2} (T/400)^{7/4} (C/2.88 \times 10^{-4})^{1/2} (A_L/2)}{p(\text{torr})w(\text{cm})[1 + (0.6 p_{DF}/p_F)]^{1/2}} \quad (34a)$$

when $m = 1/2$ and

$$\phi_e = 0.665 \frac{C_1^2}{C_2} \frac{(p/p_F)(T/400)^2 (u/4 \times 10^5)(A_T/0.1)}{p(\text{torr})w(\text{cm})[1 + (0.6 p_{DF}/p_F)]} \quad (34b)$$

when $m = 1$. The dependence of ϕ_e on physical variables is considerably different for the laminar and turbulent mixing cases except for the dependence on pw. The corresponding length of the lasing zone is, from Eqs. (30b) and (32)

$$x_e(\text{cm}) = \frac{mC_1}{C_2} \frac{(p/p_F)(T/400)^2}{0.0752 p(\text{torr})} \frac{(u/4 \times 10^5)}{[1 + (0.6 p_{DF}/p_F)]} \quad (35)$$

The lasing length is proportional to u/p , which is expected from binary scaling considerations, and is independent of w .

Similar expressions can be deduced for a cold-reaction DF laser with combustor-generated HF present in the oxidizer flow. For a DF lasing molecule, $\bar{\sigma} = 1$, $T_R = 15.6$ K, $M = 21$ g/mole, and

$$M_{O,J}^2 \times 10^{38} = 0.662 [1 + 0.045 J] \text{ erg-cm}^3 \quad (36a)$$

$$M_{v,J}^2/M_{O,J}^2 = 1 + v - 0.005 v^3 \quad (36b)$$

$$\sigma_{O,1} = 2.03 \times 10^7 (400/T)^{3/2} / \text{mole} \quad (36c)$$

Equations (36) are correlations of estimates by Herbelin that are believed to be accurate to within about 10% for $1 \leq J \leq 13$, $v \leq 6$. Consider HF and DF to be the major deactivators of $DF(v)$, approximate p_{DF} by the initial value of p_F , and include only the leading terms in Eqs. (A-19) and (A-20). Equations (32) through (35) then apply for the cold-reaction DF laser if $[1 + 0.6 (p_{DF}/p_F)]$ is replaced by $0.4 [1 + 1.6 (p_{HF}/p_F)]$, if $[1 + 0.063J]$ is replaced by $0.365 [1 + 0.045 J]$, and if $C = 2.35 \times 10^{-4}$ (corresponding to diffusion of D_2 into He) is used in Eq. (34a). For a cold-reaction DF laser, $a_v = 0, 0.10, 0.24, 0.38$, and 0.28 ; hence, $C_1 = 2.84$ and $C_3 = 4$ for $C_2 = \exp(-2 JT_R/T) \ll 1$. The product $1.641 \phi_e$ yields the laser output in terms of kilojoules per gram of fluorine for a mean output wave length of $3.837 \mu\text{m}$.

The two-level model of Mirels, Hofland, and King⁶ corresponds to the choice $v_f = a_1 = r_1 = A = \sigma_o / \sigma_1 = 1$. For this case, $C_1 = C_2 = C_3 = 1/2$, and the present results agree with those of Ref. 6[†]. For a given lasing species, scaling laws deduced from the multiple-level model differ from those deduced from the two-level model only in the dependence of C_1 , C_2 , and C_3 on T and J . The effect of the latter on laser performance is approximated, in the two-level model, by appropriate normalizations; e.g., chemical efficiency for $\zeta_D \neq 0$ is normalized to the value for $\zeta_D = 0$, and by the use of suitable mean rates; e.g., $k_{cd}^{(2)}$ was used to characterize HF collisional deactivation.

The mixing model used by Broadwell⁷ is illustrated in Fig. 5. It is shown in Appendix C that the latter leads to results that are identical with the flame-sheet-mixing model used herein if mean chemical rate are used in both models.

[†]The present oscillator solution becomes identical with the solution of Ref. 6 if the present variables $C_2 \zeta / C_1$, ϕ_e / C_1 , $C_3 G_c / C_2$, and $C_1 K_1 / C_2$ are identified with the variables ζ , η , $G_c / \sigma w [F]_o$, and K_1 in Ref. 6.

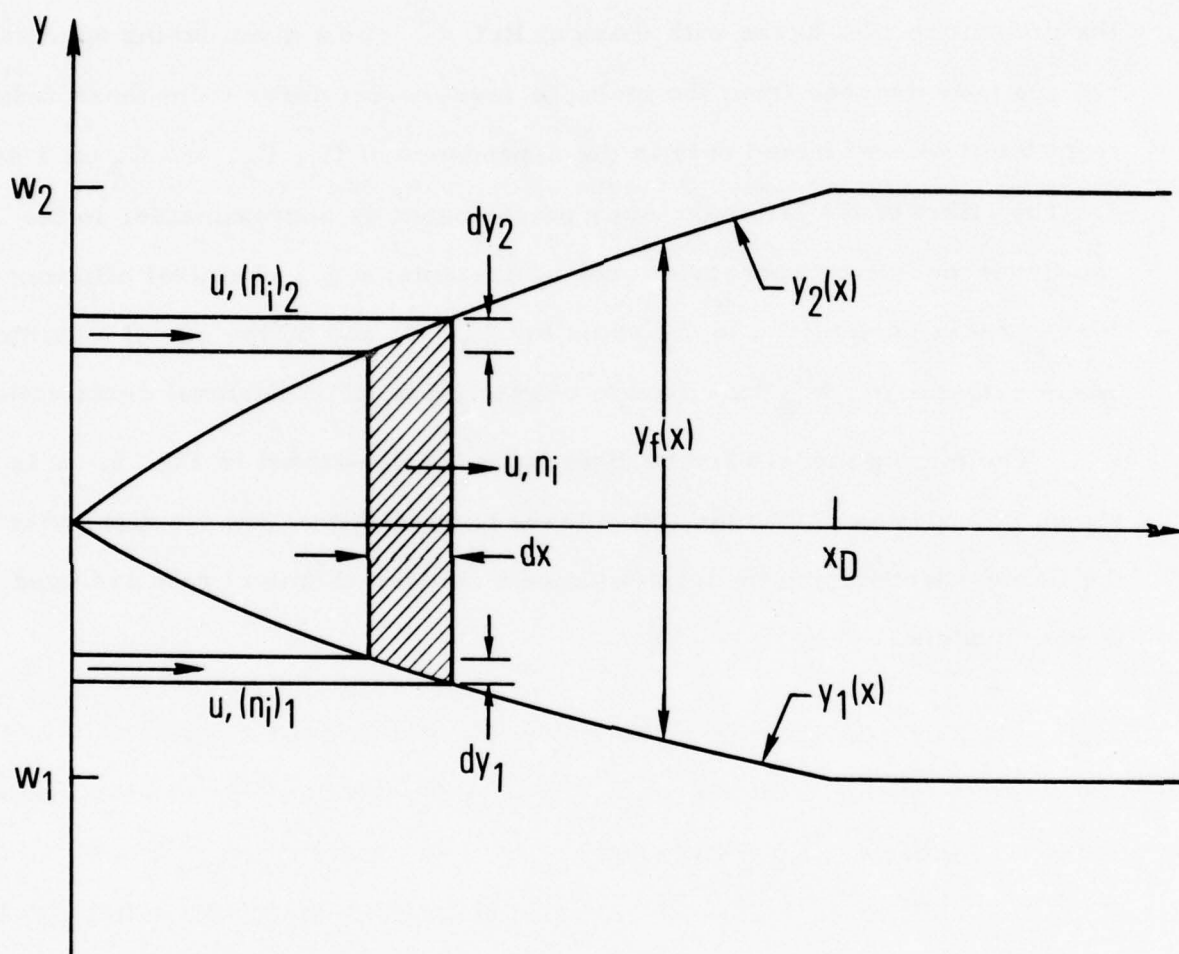


Figure 5. Mixing model of Broadwell

IV. CONCLUDING REMARKS

It is clear from Eqs. (34) that the dependence of ϕ_e on physical variables is different for laminar and turbulent flows. Hence, it is important to establish whether the flow is laminar or turbulent before applying the present results. The Reynolds number per unit length at the oxidizer nozzle exit, for a typical current laser design¹¹ is of order $R_e/\text{cm} = O(10^3)$, e.g., helium at $p = 10$ torr, $T = 300$ K, $u = 4 \times 10^5$. Most of the energy is extracted within a few centimeters of the nozzle exit.¹¹ This suggests that the mixing is laminar in the region of interest, as was, in fact, observed by Varwig¹² and by Shackleford et al.¹³ Shock-induced separation at the nozzle exit and blunt nozzle trailing edges may hasten transition to turbulence.¹² In the latter case, the mixing in the lasing region may be classified as "transitional." In these cases, the choice $m = 1/2$ or an alternative choice for $y_f = y_f(x)$ may be more appropriate than the choice $m = 1$, which implies fully developed turbulent flow.[§] Further study is needed.

It should also be noted that the simplified models of Mirels, Hofland, and King,⁶ Broadwell,⁷ and the present study neglect features of the flow

[§] Note, from Eq. (35), that Reynolds number based on lasing length is independent of pressure level. Hence, an increase in pressure level does not necessarily result in turbulent mixing in the lasing region.

that may be important in some cases. In particular, initial flow nonuniformity (because of nozzle wall boundary layer); pressure nonuniformity, i. e., shocks, edge effects, and lateral gas expansion; and heat addition effects, i. e., streamwise temperature variation effect on rates, are neglected. Appropriate mean values are needed.

APPENDIX A. REACTION MODEL

The simplified reaction model used in this report is illustrated by considering pumping and collisional deactivation reactions for a HF laser. Backward reactions are neglected.

A. PUMPING REACTION

1. COLD-REACTION LASER

The cold-reaction HF laser uses molecular hydrogen and atomic fluorine. Vibrationally excited HF is generated by the pumping reaction



where $\overline{k_p^{(v)}}$ is the rate coefficient for production of HF(v), and $\overline{k_p} = \sum_{v=0}^{v_f} \overline{k_p^{(v)}}$ is the overall rate coefficient. The rate of change of n_F along a single stream tube with velocity u , assuming a hydrogen rich mixture, is

$$u \, d n_F / dx = - \overline{k_p} \, n_{\text{H}_2} \, n_F \quad (\text{A2a})$$

$$\equiv - k_p \, n_F \quad (\text{A2b})$$

The quantity $k_p \equiv \overline{k_p} \, n_{\text{H}_2}$ has the units sec^{-1} , and a mean value is used. The reciprocal of k_p is the characteristic pumping time. If the reaction starts at x_0 with an initial concentration $(n_F)_\infty$ (Fig. 1), the downstream concentration of atomic fluorine along the stream tube is

$$n_F / (n_F)_\infty = e^{-k_p (x - x_0) / u} \quad (\text{A3})$$

Let $a_v = k_p^{(v)}/k_p$ and note $\sum_{v=0}^{v_f} a_v = 1$. From Eqs. (A1) and (A2), the vibrationally excited HF created by the pumping reaction is, for each stream tube,

$$u(d n_v/dx)_p = a_v k_p n_F \quad (A4)$$

The net rate of creation of HF(v) at a given streamwise station, due to all the stream tubes, is found by integrating Eq. (A4) between $y = 0$ and $y_f(x)$. The result, after introduction of nondimensional variables, is

$$(d N_v/d\zeta)_p = a_v K_1 N_F \quad (A5a)$$

where

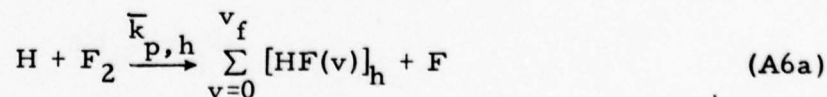
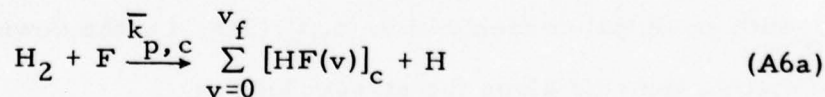
$$K_1 N_F = K_1 e^{-K_1 \zeta} \int_0^{\zeta} e^{K_1 \zeta_0} (dY_0/d\zeta_0) d\zeta_0 \quad (A5b)$$

$$= dY/d\zeta \quad (K_1 \rightarrow \infty) \quad (A5c)$$

and $n_r = (n_F)_\infty$, $Y_0 = y_f(x_0)/w$, $Y = y_f(x)/w$.

2. CHAIN-REACTION LASER

The chain-reaction HF laser uses H_2 and partially dissociated F_2 . Vibrationally excited HF is created by the chain reaction



where subscripts c and h denote cold and hot reactions, respectively, and

$$\bar{k}_{p,c} = \sum_{v=0}^{v_f} \bar{k}_{p,c}^{(v)}, \text{ and } \bar{k}_{p,h} = \sum_{v=0}^{v_f} \bar{k}_{p,h}^{(v)}. \text{ [Subscript c was omitted in Eq. (A1).]}$$

The rate of change of species along a stream tube is found from

$$\frac{d n_{H_2}}{dx} = \left(\frac{d n_F}{dx} \right)_c = - \left(\frac{d n_{ToT}}{dx} \right)_c = - \left(\frac{d n_H}{dx} \right)_c = - \frac{\bar{k}_{p,c} n_F n_{H_2}}{u} \quad (A7a)$$

$$\frac{d n_{F_2}}{dx} = \left(\frac{d n_H}{dx} \right)_h = - \left(\frac{d n_{ToT}}{dx} \right)_h = - \left(\frac{d n_F}{dx} \right)_h = - \frac{\bar{k}_{p,h} n_H n_{F_2}}{u} \quad (A7b)$$

where $n_{ToT} = \sum_{v=0}^{v_f} n_v$. It follows from Eq. (A7)

$$n_F + n_H = (n_F + n_H)_\infty \quad (A8)$$

The solution of Eqs. (A7) is found by using an approach similar to that used by Skifstad¹⁴ for the premixed laser case. In order to obtain a closed-form solution, we assume that

$$\bar{k}_{p,c} n_F = \bar{k}_{p,h} n_H \equiv k_p \quad (A9a)$$

$$(n_{H_2})_\infty = (n_{F_2})_\infty \quad (A9b)$$

It follows that, along each streamtube

$$n_{F_2} / (n_{F_2})_\infty = e^{-k_p(x-x_0)/u} \quad (A10a)$$

$$n_{ToT} / (n_{F_2})_\infty = 2 \left(1 - e^{-k_p(x-x_0)/u} \right) \quad (A10b)$$

Define $a_{v,c} = \bar{k}_{p,c}^{(v)} / \bar{k}_{p,c}$; $a_{v,h} = \bar{k}_{p,h}^{(v)} / \bar{k}_{p,h}$. The production of n_v by the pumping reaction is, then,

$$u(d n_v / dx)_p = a_v k_p n_{F_2} \quad (A11)$$

where $a_v = a_{v,c} + a_{v,h}$. The net production of n_v at each streamwise station is found by integrating Eq. (A11) between $y = 0$ and $y_f(x)$. Introduction of non-dimensional variables, with $n_r \equiv (n_{F_2})_\infty$, yields

$$(d N_v / d \zeta)_p = a_v K_1 N_{F_2} \quad (A12a)$$

where

$$K_1 N_{F_2} = K_1 e^{-K_1 \zeta} \int_0^\zeta e^{K_1 \zeta_0} (dY_0 / d\zeta_0) d\zeta_0 \quad (A12b)$$

Equations (A12) have the same form as Eqs. (A5). However, a_v , n_r , and k_p are defined differently.

The present solution is self consistent provided $(n_F)_\infty / (n_H)_\infty = \bar{k}_{p,h} / \bar{k}_{p,c}$. In most HF lasers, $(n_F)_\infty \neq 0$, $(n_H)_\infty = 0$. In these cases, the present solution becomes applicable, after a short transient, for flows with small initial F_2 dissociation. Values of n_F and n_H , after the transient, are

$$\frac{n_F}{(n_F)_\infty} = \frac{\bar{k}_{p,h}}{\bar{k}_{p,c} + \bar{k}_{p,h}} \quad \frac{n_H}{(n_F)_\infty} = \frac{\bar{k}_{p,c}}{\bar{k}_{p,c} + \bar{k}_{p,h}} \quad (A13)$$

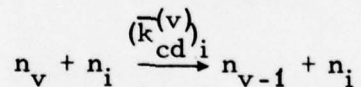
and the pumping rate for the chain reaction is, then,

$$k_p = \frac{\bar{k}_{p,c} (n_F)_\infty}{[1 + (\bar{k}_{p,c}/\bar{k}_{p,h})]} \quad (A14)$$

Denote the initial dissociation level by $\alpha = [n_F/(n_F + 2n_{F_2})]_\infty$. The ratio of the pumping rate in a chain-reaction laser to the rate in an equivalent (same net fluorine flow) cold-reaction laser is of order α . For low values of α , the parameter K_1 may be reduced to values of order one, and the chain-reaction laser will have considerably lower chemical efficiency than an equivalent cold-reaction laser.

B. COLLISIONAL DEACTIVATION

We now consider vibration-translation (v-t) deactivation of excited species and neglect vibration-vibration transfer. The v-t deactivation of n_v by species n_i , namely,



is found from

$$u \, d n_v / dx = - (\bar{k}_{cd}^{(v)})_i n_i n_v \quad (A15)$$

The deactivation of n_v by all species can be expressed

$$u \, d n_v / dx = - k_{cd}^{(v)} n_v \quad (A16a)$$

where

$$k_{cd}^{(v)} = \sum_i \left(\bar{k}_{cd}^{(v)} \right)_i n_i \quad (A16b)$$

and $k_{cd}^{(0)} = 0$. The quantity $k_{cd}^{(v)}$ is assumed to be a constant, and characteristic values of the major deactivators are used in Eq. (A16b). For arc-driven cold-reaction HF lasers,¹⁰ the major deactivator is HF (and possibly H, F). The number density of each of the latter can be characterized by $(n_F)_\infty$. For combustion-driven HF lasers,¹⁰ the introduction of major deactivation species by the combustor, e.g., DF, needs to be considered.

C. RATE COEFFICIENTS

Pumping and collisional deactivation rates for a HF laser, from Cohen,¹⁵ are repeated here for convenience. Units are $T = ^\circ K$ and $\bar{k} = \text{cm}^3 / \text{mole-sec}$. The overall pumping reaction rates [Eq. (A6)] are

$$\bar{k}_{p,c} = 1.6 \times 10^{14} e^{-805/T} \quad (A17a)$$

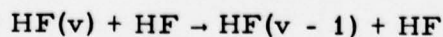
$$\bar{k}_{p,h} = 1.2 \times 10^{14} e^{-1208/T} \quad (A17b)$$

and the distributional coefficients are

$$a_{v,c} = 0, 0.17, 0.55, 0.28 \quad (v = 0, 1, 2, 3) \quad (A17c)$$

$$a_{v,h} = 0, 0, 0, 0.08, 0.13, 0.35, 0.44 \quad (v = 0, 1, \dots, 6) \quad (A17d)$$

The major collisional deactivation process in arc-driven lasers is



for which the rate coefficient is

$$\left(\overline{k}_{cd}^{(v)}\right)_{HF}^{HF*} = v \left(3 \times 10^{14} T^{-1} + 3.5 \times 10^4 T^{2.26} \right) \quad (A18)$$

The latter differs somewhat from the rate used by Mirels, Hofland, and King.⁶ Collisional deactivation of HF(v) by DF, in combustion-driven lasers, can be estimated from⁷

$$\left(\overline{k}_{cd}^{(v)}\right)_{DF}^{HF*} = v \left(1.9 \times 10^{14} T^{-1} + 1.35 \times 10^2 T^3 \right) \quad (A19)$$

Equation (A17) neglects vibration-vibration collisions, which may be significant.

The rate coefficient for the collisional deactivation of DF(v) by DF is

$$\left(\overline{k}_{cd}^{(v)}\right)_{DF}^{DF*} = v \left(1.2 \times 10^{14} T^{-1} + 1.4 \times 10^2 T^{2.96} \right) \quad (A20)$$

The rate coefficient for the deactivation of DF(v) by HF is the same as that indicated in Eq. (A19).

⁷N. Cohen, The Aerospace Corporation, private communication.

APPENDIX B. ZERO-POWER NUMBER DENSITY DISTRIBUTION

Number density distributions, in the absence of radiation, are found herein for the case $Y = (\zeta/\zeta_D)^m$, $K_1 \rightarrow \infty$, $r_v = v$, and $v_f \leq 3$. Integration of Eq. (14) yields the following results.

A. LAMINAR FLOW ($m = 1/2$)

$$\zeta_D^{1/2} N_3 = 3^{-1/2} a_3 D[(3\zeta)^{1/2}] \quad (B1a)$$

$$\zeta_D^{1/2} N_2 = 2^{-1/2} (a_2 + 3a_3) D[(2\zeta)^{1/2}] - 3^{1/2} a_3 D[(3\zeta)^{1/2}] \quad (B1b)$$

$$\begin{aligned} \zeta_D^{1/2} N_1 = & (a_1 + 2a_2 + 3a_3) D[\zeta^{1/2}] - 2^{1/2} (a_2 + 3a_3) D[(2\zeta)^{1/2}] \\ & + 3^{1/2} a_3 D[(3\zeta)^{1/2}] \end{aligned} \quad (B1c)$$

$$\zeta_D^{1/2} N_0 = \zeta^{1/2} - \zeta_D^{1/2} (N_1 + N_2 + N_3) \quad (B1d)$$

where $D[z]$ is the Dawson integral¹⁶

$$\begin{aligned} D[z] &= e^{-z^2} \int_0^z e^{z_0^2} dz_0 \\ &= z [1 - (2/3) z^2 + o(z^4)] \\ &= (2z)^{-1} [1 + (2z^2)^{-1} + o(z^{-4})] \end{aligned} \quad (B1e)$$

B. TURBULENT FLOW ($m = 1$)

$$3\zeta_D N_3 = a_3(1 - e^{-3\zeta}) \quad (\text{B2a})$$

$$2\zeta_D N_2 = a_2 + a_3 - (a_2 + 3a_3)e^{-2\zeta} + 2a_3e^{-3\zeta} \quad (\text{B2b})$$

$$\begin{aligned} \zeta_D N_1 = & a_1 + a_2 + a_3 - (a_1 + 2a_2 + 3a_3)e^{-\zeta} \\ & + (a_2 + 3a_3)e^{-2\zeta} - a_3e^{-3\zeta} \end{aligned} \quad (\text{B2c})$$

$$\zeta_D N_o = \zeta - \zeta_D(N_1 + N_2 + N_3) \quad (\text{B2d})$$

APPENDIX C. MIXING MODELS

It is now shown that, when mean values of reaction rates are used, the scheduled-mixing model of Broadwell⁷ is equivalent to the mixing model of Mirels, Hofland, and King⁶ used herein.

The mixing model of Broadwell is illustrated in Fig. 5. For a HF laser, the quantities w_1 and w_2 represent the semichannel widths of the hydrogen and the fluorine-diluent streams, respectively. Both streams have the same velocity u . The reaction zone is assumed to be bounded by two similarly shaped curves, denoted by y_1 and y_2 in Fig. 5. Fluid properties in the reaction zone depend only on x . Free-stream particles that intercept the bounding curves between station x and station $x + \Delta x$ are assumed to be uniformly distributed throughout the reaction zone. The axial distance required for all the reactants to enter the reaction zone is denoted by x_D and is equivalent to the diffusion distance in the flame sheet model. Note that w_1 and w_2 are the values of y_1 and y_2 at x_D . Although Broadwell considered only turbulent mixing with $w_1 = w_2$, we only require that y_1 and y_2 be similar in shape, i. e., $y_1/y_2 = \text{constant}$. Introduce $y_f = y_2 - y_1$. The rate of change of any species n_i in the reaction zone can be expressed as

$$u \frac{dn_i}{dx} = [(n_i)_2 \frac{dy_2}{dy_f} - (n_i)_1 \frac{dy_1}{dy_f}] \frac{u}{y_f} \frac{dy_f}{dx} - \frac{n_i u}{y_f} \frac{dy_f}{dx} + \omega_i \quad (C1)$$

where $(n_i)_1$ and $(n_i)_2$ represent the free-stream values of n_i intercepting curves y_1 and y_2 , respectively. The first term on the right side of Eq. (C1) represents

the rate of increase of n_i because of particles entering the reaction zone; the second term represents the decrease in n_i because of the lateral expansion of the reaction zone; the third term ω_i represents the rate of change of n_i because of chemical and radiative reactions. Since y_1 and y_2 are assumed to be similar in shape, a mean free-stream value of n_i , denoted $(n_i)_\infty$, can be introduced such that

$$(n_i)_\infty = [(n_i)_2 y_2 - (n_i)_1 y_1] / y_f \quad (C2)$$

Equation (C1) can then be written as

$$\frac{u}{y_f} \frac{d\{[n_i - (n_i)_\infty] y_f\}}{dx} = \omega_i \quad (C3)$$

For lasing molecules, the right side of Eq. (C3) has the same terms as the right side of Eq. (3). Introduce $w = w_2 - w_1$, $N_v = n_v y_f / w n_r$, $G_v = g_v y_f / \sigma_v w n_r$, and note $(n_v)_\infty = 0$. Equation (C3) then reduces to Eqs. (5). The term $(dN_v / d\zeta)_p$ in Eqs. (5) is found by integrating Eq. (C3) for $n_i = n_F$. The results are the same as those deduced in Appendix A.

Thus, the mixing model of Broadwell⁷ corresponds to a flame sheet model with premixed reactants [the number density being given by Eq. (C2)], a flame sheet location $y_f = y_2 - y_1$, and a diffusion distance x_D , which is evaluated by consideration of the actual diffusion process. At each axial station, number densities in the Broadwell model correspond to average values in the flame-sheet model. The equivalence requires that the coefficients of

n_v , in Eq. (3), be independent of y . Hence, the use of mean rates, at each axial station, is required in the flame-sheet model for equivalence.

REFERENCES

1. King, W. S. and Mirels, H., "Numerical Study of a Diffusion Type Chemical Laser," AIAA Journal Vol. 10, No. 12, Dec. 1972, pp. 1647-1654.
2. Thoenes, J., et. al., "Chemical Laser Analysis Development, Vol. 1, Laser and Mixing Program Theory and Users Guide," Technical Rept. RK-CR-73-2, Oct. 73, Lockheed Missiles and Space Co., Huntsville, Alabama.
3. Tripodi, R., et. al. "A Coupled Two-Dimensional Computer Analysis of CW Chemical Mixing Lasers," AIAA Paper 74-224, 1974.
4. Hofland, R. and Mirels, H., "Flame Sheet Analysis of CW Diffusion Type Chemical Laser, I. Uncoupled Radiation," AIAA Journal, Vol. 10, No. 4, April 1972, pp. 420-428.
5. Hofland, R. and Mirels, H., "Flame Sheet Analysis of CW Diffusion Type Chemical Laser, II. Coupled Radiation," AIAA Journal, Vol. 10, No. 10, Oct. 1972, pp. 1271-1280.
6. Mirels, H., Hofland, R., and King, W. S., "Simplified Model of CW Diffusion Type Chemical Laser," AIAA Journal, Vol. 11, No. 2, Feb. 1973, pp. 156-164.
7. Broadwell, J. E., "Effect of Mixing Rate on HF Chemical Laser Performance," Applied Optics, Vol. 13, No. 4, April 1974, pp. 962-967.
8. Emanuel, G. and Whittier, J. S., "Closed Form Solution to Rate Equations for an $F + H_2$ Laser Oscillator," Applied Optics, Vol. 11, No. 9, Sept. 1972, pp. 2047-2056.

9. Kwok, M. A., Giedt, R. R., and Gross, R. W. F., "Comparison of HF and DF Continuous Chemical Lasers: II. Spectroscopy," Applied Physics Letters, Vol. 16, No. 10, 15 May 1970, pp. 386-387.
10. Warren, W. R., Jr., "Chemical Lasers," Aeronautics and Astronautics, Vol. 13, No. 4, April 1975, pp. 36-49.
11. Spencer, D. J., Mirels, H., and Durran, D. A., "Performance of CW HF Chemical Laser With N₂ or He Diluent," Journal of Applied Physics, Vol. 43, No. 3, March 1972, pp. 1151-1157.
12. Varwig, R. L., "Photographic Observation of CW HF Chemical Laser Reacting Flowfield," AIAA Journal, Vol. 12, No. 10, Oct. 1974, pp. 1448-1450.
13. Shackleford, W. L., et. al., "Experimental Measurements in Supersonic Reacting F + H₂ Mixing Layers," AIAA Journal, Vol. 12, No. 8, Aug. 1974, pp. 1009-1010.
14. Skifstad, J. G., "Theory of an HF Chemical Laser," Combustion Science and Technology, Vol. 6, 1973, pp. 287-306.
15. Cohen, N., "A Review of Rate Coefficients for Reactions in the H₂ - F₂ Laser System," TR-0173 (3430)-9, Nov. 1972, The Aerospace Corp., El Segundo, Calif.
16. Abromowitz, M. and Stegun, I. A., "Handbook of Mathematical Functions," AMS 55, June 1964, National Bureau of Standards, p. 319.

SYMBOLS

$$A, A_v, A_{v,J} = e^{-2J T_R/T}$$

$$a_v = \text{fraction of particles pumped into level } v, k_p^{(v)}/k_p$$

$$C_1, C_2, C_3 = \text{functions of } J T_R/T, \text{ Eq. 25}$$

$$F_v = \text{defines } N_v \text{ in saturated oscillator, Eq. (22)}$$

$$G_c = \text{normalized gain per semichannel in optical cavity, } \sigma_v G_v / \sigma_o$$

$$G_v = \text{normalized gain per semichannel, Eq. (4)}$$

$$g_v, g_{v,J} = \text{gain per unit length on transition } v+1, J-1 \rightarrow v, J, \text{ cm}^{-1}$$

$$H_v = \text{defines effect on } N_v \text{ of } G_c \neq 0, \text{ Eq. (22)}$$

$$\Delta H = \text{net energy (joules) released by pumping reaction per mole of } n_r$$

$$\bar{I}_v, \bar{I}_{v,J} = \text{Local lasing intensity, watt/cm}^2$$

$$I_v, I_{v,J} = \text{normalized value of lasing intensity, Eq. (4)}$$

$$J = \text{rotational quantum number}$$

$$K_1 = \text{ratio of net pumping rate to } v=1 \rightarrow v=0 \text{ deactivation rate, } k_p/k_{cd}^{(1)}$$

$$k = \text{mean rate, sec}^{-1}$$

$$\bar{k} = \text{rate coefficient, cm}^3/(\text{mole-sec})$$

$$M = \text{molecular weight of excited species}$$

$$m = 1/2, 1 \text{ for laminar and turbulent flames, respectively}$$

N_{TOT} = measure of net amount of particles in levels $v = 0$ to $v = v_f$
at station x

N_i = measure of net amount of species i at station x , Eq. (4)

n_i = local number density of species i , mole/cm³

n_r = reference number density (equals $[n_F]_\infty$ and $[n_{F_2}]_\infty$ for cold
reaction and chain reaction HF lasers, respectively)

n_{sc} = number of semichannels

P = net output power, per semichannel, emitted up to station x ,
watt/cm

P_e = net oscillator output power, per semichannel, watt/cm

R_1, R_2 = reflectivity of mirrors 1 and 2

r_v = relative deactivation rate, $(k_{cd}^{(v)} + k_{sp}^{(v)})/k_{cd}^{(1)}$

T = rotational and translational temperature, °K

T_R = characteristic rotational temperature, °K

u = flow velocity in x direction, cm/sec

v = vibrational level, $v = 0, 1, \dots, v_f$

v_f = highest vibrational level considered

w = oxidizer channel semiwidth, cm (Fig. 1)

x = axial distance, cm

x_D = characteristic diffusion distance, $y_f(x_D) = w$

x_0 = flame sheet abscissa, cm

$$Y = y_f(x)/w$$

$$Y_o = y_f(x_o)/w$$

$$y_f(x) = \text{flame sheet ordinate, cm}$$

$$\epsilon = \text{mean value of } \epsilon_v$$

$$\epsilon_v = \text{energy (joules) per mole of photons for transition } v+1, J-1 \rightarrow v, J$$

$$\phi = \text{net photon output up to station } \zeta, \text{ per initial reference } (n_r)$$

$$\text{particle, } \phi = \sum_{v=0}^{v_f-1} \phi_v$$

$$\phi_v = \text{value of } \phi \text{ for single transition } v+1, J-1 \rightarrow v, J$$

$$\phi_e = \text{net photon output per initial } n_r \text{ particle for an oscillator}$$

$$\zeta = \text{normalized axial distance, } k_{cd}^{(1)} x/u$$

$$\zeta_D = \text{ratio of characteristic diffusion distance to characteristic deactivation distance, } k_{cd}^{(1)} x_D/u$$

$$\zeta_e = \text{value of } \zeta \text{ at end of lasing zone in oscillator}$$

$$\zeta_i = \text{value of } \zeta \text{ at which lasing is initiated}$$

$$\sigma_v, \sigma_{v,J} = \text{cross section for stimulated emission, Eq. (2), cm}^2/\text{mole}$$

$$\eta_c = \text{chemical efficiency, Eq. (26)}$$

Subscripts

$$cd = \text{collisional deactivation}$$

$$F, F_2 = \text{atomic or molecular fluorine, respectively}$$

i = species i

p = pumping reaction

sp = spontaneous emission

v = vibrational energy level

v or v, J = associated with transition $v + 1, J - 1 \rightarrow v, J$.

∞ = free-stream value

o = corresponding to $v = 0$ or x_o

THE IVAN A. GETTING LABORATORIES

The Laboratory Operations of The Aerospace Corporation is conducting experimental and theoretical investigations necessary for the evaluation and application of scientific advances to new military concepts and systems. Versatility and flexibility have been developed to a high degree by the laboratory personnel in dealing with the many problems encountered in the nation's rapidly developing space and missile systems. Expertise in the latest scientific developments is vital to the accomplishment of tasks related to these problems. The laboratories that contribute to this research are:

Aerophysics Laboratory: Launch and reentry aerodynamics, heat transfer, reentry physics, chemical kinetics, structural mechanics, flight dynamics, atmospheric pollution, and high-power gas lasers.

Chemistry and Physics Laboratory: Atmospheric reactions and atmospheric optics, chemical reactions in polluted atmospheres, chemical reactions of excited species in rocket plumes, chemical thermodynamics, plasma and laser-induced reactions, laser chemistry, propulsion chemistry, space vacuum and radiation effects on materials, lubrication and surface phenomena, photosensitive materials and sensors, high precision laser ranging, and the application of physics and chemistry to problems of law enforcement and biomedicine.

Electronics Research Laboratory: Electromagnetic theory, devices, and propagation phenomena, including plasma electromagnetics; quantum electronics, lasers, and electro-optics; communication sciences, applied electronics, semiconducting, superconducting, and crystal device physics, optical and acoustical imaging; atmospheric pollution; millimeter wave and far-infrared technology.

Materials Sciences Laboratory: Development of new materials; metal matrix composites and new forms of carbon; test and evaluation of graphite and ceramics in reentry; spacecraft materials and electronic components in nuclear weapons environment; application of fracture mechanics to stress corrosion and fatigue-induced fractures in structural metals.

Space Sciences Laboratory: Atmospheric and ionospheric physics, radiation from the atmosphere, density and composition of the atmosphere, aurorae and airglow; magnetospheric physics, cosmic rays, generation and propagation of plasma waves in the magnetosphere; solar physics, studies of solar magnetic fields; space astronomy, x-ray astronomy; the effects of nuclear explosions, magnetic storms, and solar activity on the earth's atmosphere, ionosphere, and magnetosphere; the effects of optical, electromagnetic, and particulate radiations in space on space systems.

THE AEROSPACE CORPORATION
El Segundo, California